Current-induced pseudospin polarization in silicene*

Wang Lei(王 磊) and Zhu Guo-Bao(朱国宝)†

Department of Physics and Electronic Engineering, Heze University, Heze 274015, *China*

(Received 21 March 2014; revised manuscript received 23 April 2014; published online 16 July 2014)

The pseudospin polarization induced by an external electric field in silicene in the presence of weakly spin-independent impurities is considered theoretically in the linear response regime based on Green's function method. We study the effects of the interplay between the sublattice potential and the intrinsic spin orbit coupling on the pseudospin polarization. We show that the pseudospin polarization perpendicular to the electric field is independent of the impurity parameter, while the pseudospin polarization in the direction of the electric field is sensitive to the impurity parameter. The dependences of the pseudospin polarizations on the chemical potential are studied.

Keywords: silicene, pseudospin polarization, Green's function

PACS: 85.75.–d, 71.70.Ej, 72.80.Vp **DOI:** 10.1088/1674-1056/23/9/098503

1. Introduction

Silicene is a monolayer of silicon atoms forming a two-dimensional honeycomb lattice with buckled sublattices of A sites and B sites. This novel two-dimensional material has attracted considerable theoretical and experimental attention [1–13] since it was first successfully synthesized.[14–19] Due to its hexagonal lattice structure, electrons in silicene obey the Dirac equation around the K and K' points of the Brillouin zone, which is similar to the case of graphene. However, silicene has a large spin–orbit gap compared to graphene and the mass of the Dirac electrons in silicene is controllable by an external electric field due to its buckled structure. These characteristics make silicene a promising candidate for a range of applications in devices and nanoelectronics.

Pseudospintronics is a form of electronics based upon the manipulation of pseudospin, which is analogous to the control of physical spin in spintronics. Pseudospin plays an essential role in the optical and transport properties of materials. In a honeycomb lattice, the sublattice degree of freedom is referred to as a pseudospin; that is, denoting the state on the A (B) sublattice as the up (down) state of pseudospin. Recently, the manipulation of pseudospin in a pseudospintronic device has been a popular topic in the study of Dirac material-based electronic devices.[20–27] San-Jose *et al.*[20] first proposed the concept of graphene-based pseudospintronics. They manipulated the valley pseudospin in bilayer graphene materials. Zhou[22] proposed a method to generate and manipulate the pseudospin polarization in a monolayer graphene by manipulating the strength, the frequency, and especially the polarization orientation of the field. Trushin[25] showed that the pseudospin can be efficiently controlled by means of electron–electron interactions. In particular, they found that an out-of-plane pseudospin component can occur and that it leads to a zero-field Hall current, as well as leading to a polarization-sensitive interband optical absorption. Theoretically, these are both routes toward the intrinsic pseudospin polarization. In this paper, we study the effects of the interplay between the sublattice potential (out-of-plane pseudospin component) and the intrinsic spin orbit coupling on the current-induced pseudospin polarization in silicene in the presence of weakly spin-independent impurities.

The rest of this paper is organized as follows. In Section 2, we present a brief account of the effective Hamiltonian and a general formula for the current-induced pseudospin polarization. In Section 3, the analytical and numerical results of the current-induced pseudospin polarizations with different parameters are presented. Our conclusions are given in Section 4.

2. Theory and model

2.1. Effective Hamiltonian

The low-energy physics of silicene can be captured by the following simple low-energy Hamiltonian:[2–9]

$$\hat{H}_0 = \hbar v_{\rm F}(\eta p_x \hat{\sigma}_x + p_y \hat{\sigma}_y) - \eta \frac{1}{2}\Delta_{\rm so}\hat{s}_z\hat{\sigma}_z + \frac{1}{2}\Delta_z\hat{\sigma}_z, \qquad (1)$$

where $\eta = \pm 1$ correspond to the K and K' points, respectively; $\hat{\boldsymbol{\sigma}} = (\hat{\sigma}_x, \hat{\sigma}_y, \hat{\sigma}_z)$ are the Pauli matrices associated with the sublattice pseudospin; $\hat{s}_z$ is the Pauli matrix associated with the electron's spin; $v_{\rm F}$ is the Fermi velocity in silicene; and $p_{x,y}$ are components of the momentum measured relative to the K/K' point. We have set $\hbar = v_{\rm F} = 1$ throughout this paper for simplicity. The first term is the familiar graphene-type Dirac Hamiltonian, which arises from the nearest-neighbor hopping. The second term represents the effective spin–orbit coupling.

*Project supported by the Shandong Young Scientists Award Fund, China (Grant No. 2012CL001).

†Corresponding author. E-mail: zhuguobao@gmail.com

© 2014 Chinese Physical Society and IOP Publishing Ltd

The final term is associated with the on-site potential difference between the two sublattices.

In the above Hamiltonian, the K and K' valleys are decoupled. Therefore, we can solve the electronic eigenequation and the pseudospin polarization in the K valley. The eigenvalues of the Hamiltonian are given by

$$E(\tau,s)=\tau\sqrt{p^2+\frac{1}{4}(\Delta_z+s\Delta_{\rm so})^2}, \tag{2}$$

where $\tau=\pm$ refer to the conduction and the valence bands, and $s=\mp$ corresponds to the spin-up and the spin-down electrons. The corresponding eigenvectors take the following form:

$$\begin{aligned}U(\tau,s)=&\left[\frac{1-s}{2}\cos\left(\frac{\theta_s}{2}+\frac{\pi(1-\tau)}{4}\right)e^{i\varphi},\right.\\&\frac{1-s}{2}\sin\left(\frac{\theta_s}{2}+\frac{\pi(1-\tau)}{4}\right),\\&\frac{1+s}{2}\cos\left(\frac{\theta_{-s}}{2}+\frac{\pi(1-\tau)}{4}\right)e^{i\varphi},\\&\left.\frac{1+s}{2}\sin\left(\frac{\theta_{-s}}{2}+\frac{\pi(1-\tau)}{4}\right)\right]^{\rm T},\end{aligned} \tag{3}$$

where superscript T denotes the transpose of the matrix, $\cos\theta_\pm=\frac{\Delta_\pm}{\sqrt{p^2+\Delta_\pm^2}}$, $\Delta_\pm=(\Delta_z\pm\Delta_{\rm so})/2$, and $\cos\varphi=p_x/p$. The effect of the interplay of $\Delta_{\rm so}$ and Δ_z on the energy spectrum is shown in Fig. 1, the corresponding eigenvectors of the energy spectrum are also marked. The Dirac mass term for the K valley in the bulk silicene is given by $-\Delta_{\rm so}\hat{s}_z/2+\Delta_z/2$. In addition, $\Delta_{\rm so}=\Delta_z$ (see Fig. 1(b)) is a critical point where the energy gap closes. The sign of the mass term can be changed by tuning the sublattice potential. This represents the evolution of the gap (closing and reopening), and the inversion between the conduction (blue curve in Fig. 1(a) and red curve in Fig. 1(c)) and the valence bands (red curve in Fig. 1(a) and blue curve in Fig. 1(c)). Therefore, a topological phase transition exists. The system is a topological insulator for $\Delta_{\rm so}<\Delta_z$, while it is a nontopological insulator for $\Delta_{\rm so}>\Delta_z$.

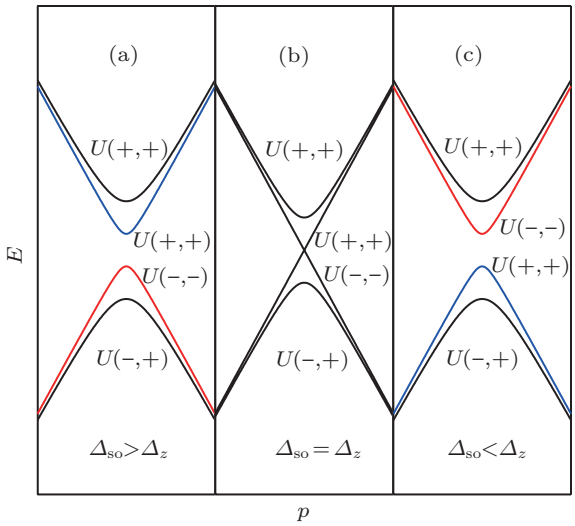


Fig. 1. (color online) Dependence of the energy spectrum on the interlay between $\Delta_{\rm so}$ and Δ_z: (a) $\Delta_{\rm so}>\Delta_z$, (b) $\Delta_{\rm so}=\Delta_z$, and (c) $\Delta_{\rm so}<\Delta_z$. Here $U(\pm,\pm)$ (see Eq. 3) are the corresponding eigenvectors of the energy spectrum. The colors are used to show the inversion between conduction and valence bands.

Now we consider spin-independent impurities $\hat{H}_{\rm imp}=\sum_{\boldsymbol{r}_{\rm imp}}u_{\rm imp}\delta(\boldsymbol{r}-\boldsymbol{r}_{\rm imp})$. The self-energy can be calculated from

$$\hat{\Sigma}^{\rm r,a}=n_{\rm imp}u_{\rm imp}^2\int\frac{{\rm d}^2p}{(2\pi)^2}g_\omega^{\rm r,a}, \tag{4}$$

where $n_{\rm imp}$ is the concentration of the impurities, and $g_\omega^{\rm r,a}=\left[\omega-\hat{H}_0-\hat{\Sigma}^{\rm r,a}\right]^{-1}$. In the following, we suppose that the impurities are dilute, so that the self-consistent Born approximation is equivalent to the Born approximation. We then obtain the self-energy as

$$\begin{aligned}\hat{\Sigma}^{\rm r,a}=&\mp i\frac{n_{\rm imp}u_{\rm imp}^2}{4}\sum_{\alpha,\beta=\pm}\frac{1}{2}\beta\theta(\beta\omega-\Delta_\alpha)\\&\times[\hat{s}_0+\alpha\hat{s}_z][\omega\hat{\sigma}_0+\Delta_\alpha\hat{\sigma}_z],\end{aligned} \tag{5}$$

where $\theta(x)$ is the step function. We here assume that the system is in the weak scattering regime and that the real part of the self-energy can be neglected.

2.2. Current-induced pseudospin polarization

In this section, we will present the general formula of the pseudospin polarization in response to a dc electric field.[28,29] When we consider a dc external field, it is easier to introduce a field oscillating with frequency Ω and then take the limit $\Omega\to0$. When an external field is present, the current induced interaction term reads $V(t)=-\boldsymbol{j}\cdot\boldsymbol{A}(t)$, where $\boldsymbol{j}$ is the current operator and the vector potential $\boldsymbol{A}(t)$ satisfies $\boldsymbol{E}(t)=-\partial_t\boldsymbol{A}(t)$. The current operator is given by $j_x=-e\dot{x}=-\eta e\hat{\sigma}_x$ and $j_y=-e\dot{y}=-e\hat{\sigma}_y$. When the electric field is in the $+y$ direction, the perturbation term (interaction term) yields $V(t)=-ieE_y e^{i\Omega t}\hat{\sigma}_y/\Omega$, whose Fourier transform is $V_\Omega=-ieE_y\hat{\sigma}_y/\Omega$. By using the Dyson equation[30] $G^<=g^<+g^{\rm r}VG^<+g^<VG^{\rm a}$, we obtain

$$\begin{aligned}G^<=&\,g_\omega^<+f(\omega+\Omega)g_\omega^{\rm r}V_\Omega(g_{\omega+\Omega}^{\rm a}-g_{\omega+\Omega}^{\rm r})\\&+f(\omega)(g_\omega^{\rm a}-g_\omega^{\rm r})V_\Omega g_{\omega+\Omega}^{\rm r},\end{aligned} \tag{6}$$

where $f(x)$ is the Fermi distribution function and $g_\omega^{<,r,a}$ are the lesser, retarded, and advanced Green's functions,[31–34] respectively. By expanding the Fermi distribution function and Green's functions in terms of Ω to the linear order, we obtain

$$\begin{aligned}G^<=&\,g_\omega^<+f(\omega)\left[g_\omega^{\rm a}V_\Omega g_\omega^{\rm a}-{\rm a}\leftrightarrow{\rm r}\right]\\&+\Omega\{f(\omega)\left[g_\omega^{\rm a}V_\Omega\partial_\omega g_\omega^{\rm a}-{\rm a}\leftrightarrow{\rm r}\right]\\&+\partial_\omega f(\omega)g_\omega^{\rm r}V_\Omega\left[g_\omega^{\rm a}-g_\omega^{\rm r}\right]\}.\end{aligned} \tag{7}$$

In the above expansion, the $g_\omega^{\rm r,a}V_\Omega\partial_\omega g_\omega^{\rm r,a}$ terms do not contribute to the physical quantities.[35,36] Furthermore, V_Ω can

be written in the form of the derivative of the Hamiltonian $V_\Omega = -\mathrm{i}eE_y\partial_{p_y}\hat{H}_0/\Omega$, hence we have $\int \mathrm{d}^2p g^{\mathrm{r,a}}_\omega V_\Omega g^{\mathrm{r,a}}_\omega \propto \int \mathrm{d}^2p \partial_{p_y} g^{\mathrm{r,a}}_\omega = 0$. Therefore, only the $g^{\mathrm{r}}_\omega V_\Omega g^{\mathrm{a}}_\omega$ term contributes to the result. The pseudospin polarization at zero temperature can be calculated from the formula

$$\begin{aligned}\langle S_i\rangle &= \frac{1}{\mathrm{i}}\int\frac{\mathrm{d}\omega}{2\pi}\int\frac{\mathrm{d}^2p}{(2\pi)^2}\mathrm{Tr}\left[\Lambda_i G^<\right]\\ &= \frac{1}{\mathrm{i}}\int\frac{\mathrm{d}\omega}{2\pi}\int\frac{\mathrm{d}^2p}{(2\pi)^2}\Omega\partial_\omega f(\omega)\,\mathrm{Tr}\left[\Lambda_i g^{\mathrm{r}}_\omega V_\Omega g^{\mathrm{a}}_\omega\right], \quad (8)\end{aligned}$$

where $\Lambda_{x,y} = \hbar\hat{s}_0\otimes\hat{\sigma}_{x,y}/2$, and $\hat{s}_0$ is a 2×2 unit matrix in the spin space.

3. Analytical and numerical results

In this section, we give the formula for the current-induced pseudospin polarization in silicene based on Eq. (8). We will limit ourselves to the negative chemical potential case. The results can be easily generalized to the case when the chemical potential is positive due to the particle–hole symmetry.[37] The Hamiltonian can be decoupled into two 2×2 blocks (see Eqs. (1) and (5)). This means that the Green's functions have a block form in the spin space. Therefore, the Green's functions can be expanded in the pseudospin Pauli matrix in two (spin) subspaces; that is,

$$g^{\mathrm{r,a}}_\omega = \begin{pmatrix} g^{\mathrm{r0,a0}}_{\omega\uparrow}\hat{\sigma}_0 + \sum\limits_{l=x,y,z} g^{\mathrm{rl,al}}_{\omega\uparrow}\hat{\sigma}_l & 0 \\ 0 & g^{\mathrm{r0,a0}}_{\omega\downarrow}\hat{\sigma}_0 + \sum\limits_{l=x,y,z} g^{\mathrm{rl,al}}_{\omega\downarrow}\hat{\sigma}_l \end{pmatrix}, \quad (9)$$

where

$$g^{\mathrm{r}}_{\omega\uparrow/\downarrow} = \left[\omega - \Gamma^0_\mp - \hbar v_{\mathrm{F}}(\eta p_x\hat{\sigma}_x + p_y\hat{\sigma}_y) - (\Delta_\mp + \Gamma^z_\mp)\hat{\sigma}_z\right]^{-1},$$

$g^{\mathrm{a}} = g^{\mathrm{r}\dagger}$, and $g^{\mathrm{rl}}_{\omega\uparrow/\downarrow} = \frac{1}{2}\{g^{\mathrm{r}}_{\omega\uparrow/\downarrow}, \hat{\sigma}_l\}$, $l = 0,x,y,z$. From Eq. (5), we obtain

$$\Gamma^0_\mp = -\mathrm{i}\frac{n_{\mathrm{imp}}u^2_{\mathrm{imp}}}{4}\sum_{\beta=\pm}\frac{1}{2}\beta\theta(\beta\omega - \Delta_\mp)\omega$$

and

$$\Gamma^z_\mp = -\mathrm{i}\frac{n_{\mathrm{imp}}u^2_{\mathrm{imp}}}{4}\sum_{\beta=\pm}\frac{1}{2}\beta\theta(\beta\omega - \Delta_\mp)\Delta_\mp.$$

In the stationary limit, $\omega\to 0$, straightforward calculations show that the current-induced pseudospin polarizations at zero temperature are

$$\begin{aligned}\langle S_x\rangle &= \frac{\mathrm{i}eE_y}{\pi}\int\frac{\mathrm{d}^2p}{(2\pi)^2}\\ &\quad\times\left[g^{\mathrm{r0}}_{\mu\uparrow}g^{\mathrm{az}}_{\mu\uparrow} - g^{\mathrm{rz}}_{\mu\uparrow}g^{\mathrm{a0}}_{\mu\uparrow} + g^{\mathrm{r0}}_{\mu\downarrow}g^{\mathrm{az}}_{\mu\downarrow} - g^{\mathrm{rz}}_{\mu\downarrow}g^{\mathrm{a0}}_{\mu\downarrow}\right], \quad (10)\\ \langle S_y\rangle &= \frac{eE_y}{\pi}\int\frac{\mathrm{d}^2p}{(2\pi)^2}\\ &\quad\times\left[g^{\mathrm{r0}}_{\mu\uparrow}g^{\mathrm{a0}}_{\mu\uparrow} - g^{\mathrm{rz}}_{\mu\uparrow}g^{\mathrm{az}}_{\mu\uparrow} + g^{\mathrm{r0}}_{\mu\downarrow}g^{\mathrm{0z}}_{\mu\downarrow} - g^{\mathrm{rz}}_{\mu\downarrow}g^{\mathrm{az}}_{\mu\downarrow}\right], \quad (11)\end{aligned}$$

where μ is the chemical potential, which can be controlled by an external gate voltage. In the weak scattering limit,[38] we obtain

$$\begin{aligned}\langle S_x\rangle &= -\frac{eE_y}{2\pi}\sum_{\alpha=\pm}\frac{\cos\theta_\alpha}{1+\cos^2\theta_\alpha}\bigg|_{p=p_{\mathrm{F}}}, \quad (12)\\ \langle S_y\rangle &= \frac{eE_y}{2\pi}\frac{v^2_{\mathrm{F}}}{n_{\mathrm{imp}}u^2_{\mathrm{imp}}}\sum_{\alpha=\pm}\frac{\sin^2\theta_\alpha}{1+\cos^2\theta_\alpha}\bigg|_{p=p_{\mathrm{F}}}, \quad (13)\end{aligned}$$

where p_{F} is the Fermi momentum.

Based on the above formula, we note that the current-induced pseudospin polarization is a linear function of the electric field, which is obvious in the linear response regime. The current-induced pseudospin polarization perpendicular to the electric field ($\langle S_x\rangle$) is independent of the impurity parameter $n_{\mathrm{imp}}u^2_{\mathrm{imp}}$, while the current-induced pseudospin polarization in the direction of the electric field ($\langle S_y\rangle$) is sensitive to the impurity parameter. Moreover, we note that $\langle S_x\rangle = -eE_y/(2\pi)$ in the topological phase ($\Delta_{\mathrm{so}} < \Delta_z$) and $\langle S_x\rangle = 0$ in the nontopological phase ($\Delta_{\mathrm{so}} > \Delta_z$) when μ locates in the gap region, while $\langle S_y\rangle = 0$ in the two phases.

When μ departs from the top of the valence band, we obtain

$$\langle S_x\rangle = -\frac{eE_y}{2\pi}\left[\frac{1}{2} - \frac{2\mu(\Delta_z - \Delta_{\mathrm{so}})}{4\mu^2 + (\Delta_z - \Delta_{\mathrm{so}})^2}\right]$$

and

$$\langle S_y\rangle = \frac{eE_y}{2\pi}\frac{v^2_{\mathrm{F}}}{n_{\mathrm{imp}}u^2_{\mathrm{imp}}}\frac{4\mu^2 - (\Delta_z - \Delta_{\mathrm{so}})^2}{4\mu^2 + (\Delta_z - \Delta_{\mathrm{so}})^2}$$

for

$$-\frac{|\Delta_z + \Delta_{\mathrm{so}}|}{2} < \mu < -\frac{|\Delta_z - \Delta_{\mathrm{so}}|}{2}.$$

For $\mu < -|\Delta_z + \Delta_{\mathrm{so}}|/2$,

$$\langle S_x\rangle = \frac{eE_y}{2\pi}\left[\frac{2\mu(\Delta_z + \Delta_{\mathrm{so}})}{4\mu^2 + (\Delta_z + \Delta_{\mathrm{so}})^2} + \frac{2\mu(\Delta_z - \Delta_{\mathrm{so}})}{4\mu^2 + (\Delta_z - \Delta_{\mathrm{so}})^2}\right],$$

and

$$\begin{aligned}\langle S_y\rangle &= \frac{eE_y}{2\pi}\frac{v^2_{\mathrm{F}}}{n_{\mathrm{imp}}u^2_{\mathrm{imp}}}\left[\frac{4\mu^2 - (\Delta_z - \Delta_{\mathrm{so}})^2}{4\mu^2 + (\Delta_z - \Delta_{\mathrm{so}})^2}\right.\\ &\quad\left.+\frac{4\mu^2 - (\Delta_z + \Delta_{\mathrm{so}})^2}{4\mu^2 + (\Delta_z + \Delta_{\mathrm{so}})^2}\right].\end{aligned}$$

The variations of $\langle S_x\rangle$ and $\langle S_y\rangle$ with the chemical potential are complex and are shown in Figs. 2 and 3, respectively, for specific values of the interplay parameter $\gamma = \Delta_{\mathrm{so}}/\Delta_z$. Figure 2

shows that when μ decreases further, $\langle S_x\rangle$ reaches a minimum at some point in the nontopological phase $\gamma > 1$, which depends on the interplay parameter, and then increases with a further decrease in μ. Meanwhile, $\langle S_x\rangle$ only increases with a decrease in μ in the topological phase $\gamma < 1$. Finally, $\langle S_x\rangle = 0$ at $|\mu| \gg (\Delta_{so} + \Delta_z)/2$. Figure 3 shows that $\langle S_y\rangle$ increases with increasing μ, in both topological and nontopological phases, and $\langle S_y\rangle = \frac{eE_y}{\pi}\frac{v_F^2}{n_{imp}u_{imp}^2}$ for $|\mu| \gg (\Delta_{so} + \Delta_z)/2$.

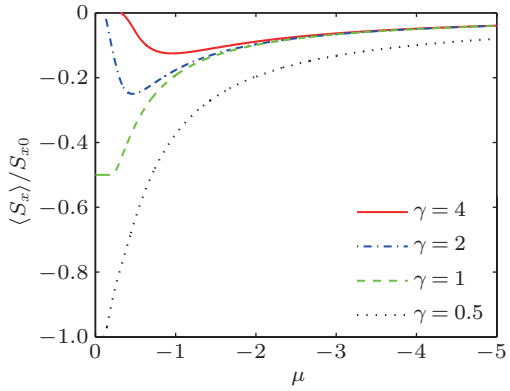


Fig. 2. (color online) The current-induced pseudospin polarization $\langle S_x\rangle$ in units of $S_{x0} = eE_y/(2\pi)$ as a function of the chemical potential μ for indicated values $\gamma = \Delta_{so}/\Delta_z$.

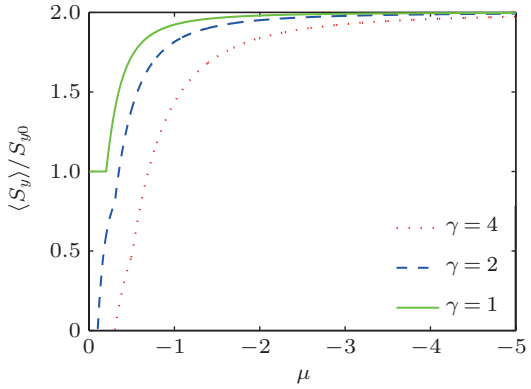


Fig. 3. (color online) The current-induced pseudospin polarization $\langle S_y\rangle$ in units of $S_{y0} = \frac{eE_y}{2\pi}\frac{v_F^2}{n_{imp}u_{imp}^2}$ as a function of the chemical potential μ for indicated values $\gamma = \Delta_{so}/\Delta_z$.

Figure 4 presents the density plots of the current-induced pseudospin polarizations $\langle S_x\rangle$ and $\langle S_y\rangle$ as a function of the chemical potential μ and the interplay parameter γ. The minima in $\langle S_x\rangle$ at $\gamma > 1$ are clearly seen in Fig. 4(a) for a constant γ when the chemical potential is below the top of the valence band. The gradual increase of $\langle S_x\rangle$ at $\gamma < 1$ can also be found. Figure 4(b) makes the results from Fig. 3 more obvious. The two white lines in Fig. 4(a) are determined by Δ_{so} and Δ_z, which stand for the valence band edge. When the constant μ locates at the interval of the two tops of the valence bands, $\langle S_x\rangle$ can be tuned from S_{x0} to 0. At constant and large values of μ, $\langle S_x\rangle$ and $\langle S_y\rangle$ become independent of Δ_{so} and Δ_z when the two valence bands are occupied.

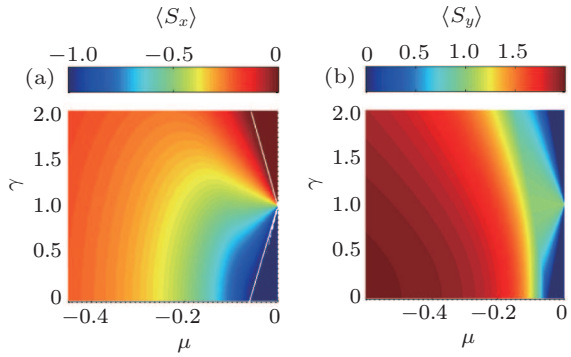


Fig. 4. (color online) The current-induced pseudospin polarization as a function of the chemical potential μ and the interplay parameter $\gamma = \Delta_{so}/\Delta_z$: (a) $\langle S_x\rangle$ in units of $S_{x0} = eE_y/(2\pi)$, (b) $\langle S_y\rangle$ in units of $S_{y0} = \frac{eE_y}{2\pi}\frac{v_F^2}{n_{imp}u_{imp}^2}$.

4. Discussion and conclusion

In summary, we have analyzed the current-induced pseudospin polarization in silicene in the presence of weakly spin-independent impurities. We have used the Green's function method to derive general formulas for the current-induced pseudospin polarization. The dependences of the current-induced pseudospin polarization on the chemical potential, and the interplay of the sublattice potential and the intrinsic spin orbit coupling are studied. The current-induced pseudospin polarization is shown to be in the silicene plane, and the polarization perpendicular to the electric field ($\langle S_x\rangle$) is independent of the impurity parameter, while the polarization in the direction of the electric field ($\langle S_y\rangle$) is sensitive to the impurity parameter. In nontopological phases, $\langle S_x\rangle$ reaches a minimum at a certain chemical potential. The position of the point changes with the sublattice potential and the intrinsic spin orbit coupling. At large $|\mu| \gg (\Delta_{so} + \Delta_z)/2$, $\langle S_x\rangle$ and $\langle S_y\rangle$ are independent of the sublattice potential and the intrinsic spin orbit coupling.

References

[1] Topsakal M and Ciraci S 2010 *Phys. Rev. B* **81** 024107
[2] Liu C C and Yao Y G 2011 *Phys. Rev. Lett.* **107** 076802
[3] Liu C C and Yao Y G 2011 *Phys. Rev. B* **84** 195430
[4] Pan H, Li Z, Liu C C, Zhu G, Qiao Z and Yao Y 2014 *Phys. Rev. Lett.* **112** 106802
[5] Chen N and Wu K H 2013 *Physics* **42** 604
[6] Ezawa M 2012 *Phys. Rev. Lett.* **109** 055502
[7] Ezawa M 2012 *New J. Phys.* **14** 033003
[8] Ezawa M 2012 *Phys. Rev. B* **86** 161407
[9] Tabert C J and Nicol E J 2013 *Phys. Rev. Lett.* **110** 197402
[10] Ni Z, Liu Q, Tang K, Zheng J, Zhou J, Qin R, Gao Z, Yu D and Lu J 2012 *Nano Lett.* **12** 113
[11] Stille L, Tabert C J and Nicol E J 2012 *Phys. Rev. B* **86** 195405
[12] Ezawa M 2013 *Phys. Rev. Lett.* **110** 026603
[13] Tahir M and Schwingenschögl U 2013 *Sci. Rep.* **3** 1075
[14] Lalmi B, Oughaddou H, Enriquez H, Kara A, Vizzini S, Ealet B and Aufray B 2010 *Appl. Phys. Lett.* **96** 223109
[15] Padova P De, Quaresima C, Ottaviani C, Sheverdyaeva P M, Moras P, Carbone C, Topwal D, Olivieri B, Kara A, Oughaddou H, Aufray B and Lay G Le 2010 *Appl. Phys. Lett.* **96** 261905
[16] Padova P De, Quaresima C, Olivieri B, Perfetti P and Lay G Le 2011 *Appl. Phys. Lett* **98** 081909

[17] Vogt P, Padova P De, Quaresima C, Avila J, Frantzeskakis E, Asensio M C, Resta A, Ealet B and Lay G Le 2012 *Phys. Rev. Lett.* **108** 155501
[18] Lin C L, Arafune R, Kawahara K, Tsukahara N, Minamitani E, Kim Y, Takagi N and Kawai M 2012 *Appl. Phys. Express* **5** 045802
[19] Fleurence A, Friedlein R, Ozaki T, Kawai H, Wang Y and Yamada-Takamura Y 2012 *Phys. Rev. Lett.* **108** 245501
[20] San-Jose P, Prada E, McCann E and Schomerus H 2009 *Phys. Rev. Lett.* **102** 247204
[21] Liu W, MacDonald A H and Culcer D 2013 *Phys. Rev. B* **87** 085408
[22] Zhou J 2008 arXiv: 0807.0667v1[cond-mat]
[23] Xia F, Farmer D B, Lin Y and Avouris P 2010 *Nano Lett.* **10** 715
[24] Min H, Borghi G, Polini M and MacDonald A H 2008 *Phys. Rev. B* **77** 041407(R)
[25] Trushin M and Schliemann J 2011 *Phys. Rev. Lett.* **107** 156801
[26] Majidi L and Zareyan M 2011 *Phys. Rev. B* **83** 115422
[27] Jia S W, Wang J T, Yang Y L and Bai C X 2013 *Chin. Phys. B* **22** 087408
[28] Xu J, Zhan S C and Shangguan W Z 2005 *Chin. Phys.* **14** 2093
[29] Yan W X and Li X Rong 2006 *Chin. Phys.* **15** 822
[30] Haug H and Jauho H P 1998 *Quantum Kinetics in Transport and Optics of Semiconductors* (Heidelberg: Springer-Verlag)
[31] Pan W Y and Li K 2002 *Chin. Phys.* **11** 1245
[32] Ren X R, Teng S Y, Xu Z Zhan, Cheng C F, Liu M and Liu C X 2004 *Acta Phys. Sin.* **53** 427 (in Chinese)
[33] Ni J and Dai Z H 2005 *Acta Phys. Sin.* **54** 3342 (in Chinese)
[34] Liu G B and Liu B G 2009 *Chin. Phys. B* **18** 5047
[35] Sinitsyn N A, MacDonald A H, Jungwirth T, Dugaev V K and Sinova J 2007 *Phys. Rev. B* **75** 045315
[36] Nagaosa N, Sinova J, Onoda S, MacDonald A H and Ong N P 2010 *Rev. Mod. Phys.* **82** 1539
[37] Yang S A, Pan H, Yao Y and Niu Q 2011 *Phys. Rev. B* **83** 125122
[38] Nunner T S, Sinitsyn N A, Borunda M F, Dugaev V K, Kovalev A A, Abanov A, Timm C, Jungwirth T, Inoue J, MacDonald A H and Sinova J 2007 *Phys. Rev. B* **76** 235312